# Effects of M/A on the Mechanical Properties of Microalloyed Steels

Martensite/retained austenite, or M/A, is a second-phase constituent in the microstructure of steel. M/A has been observed in steel products processed through different routes. M/A constituent has a strong effect on the mechanical properties of steel. Understanding its effect is very important in order to avoid any negative impact on the performance of steel. In this article, the effects of M/A on the mechanical properties of several microalloyed steels will be discussed.

Authors

Dengqi Bai (left), Principal Research Engineer, SSAB Americas R&D, Muscatine, Iowa, USA
dengqi.bai@ssab.com

Jacob Ecklund (right), Staff Metallurgist, SSAB Iowa Inc., Muscatine, Iowa, USA
jake.ecklund@ssab.com

## Introduction

It is well known that the microstructure of a given steel determines its mechanical properties. Commonly known microstructures in steel include ferrite, pearlite, bainite and martensite. These microstructures have been extensively studied and their effects on the mechanical properties of steel are well understood. For applications where formability is the critical parameter, a microstructure providing low strength and good ductility, such as polygonal ferrite, is usually the choice. For applications where wear resistance is required, bainite or martensite should be considered. Steels for special applications require the development of complex microstructures to meet the demanding performance. Steel grades such as dual-phase (DP) and transformation-induced plasticity (TRIP) have been developed for automotive applications where high strength and good formability are required.[1–5] Similarly, in modern low-carbon microalloyed steels, particularly those for line pipe applications, microstructures have become more complex to meet some stringent performance requirements. For instance, for high-strength line pipe grades, such as X100 and X120, to improve the strain-aging resistance of these steels, M/A was introduced in a base microstructure of bainite.[6–9] In a recent study by Bai et al., the effect of steel chemistry on the M/A formation in two line pipe steels was examined.[10] Their study showed that a small change in the concentrations of some dissolved elements can result in a noticeable change in the volume fraction of M/A, and hence the mechanical properties of the steels.

As a microstructural constituent, M/A has been observed in many steels. Depending on the size, morphology, volume fraction and crystal structure, the M/A constituent can have very different effects on the mechanical properties of steel, as shown by the microstructures in Fig. 1 and stress-strain curves in Fig. 2. For a steel with a microstructure consisting of polygonal ferrite and pearlite, such as the microstructure shown in Fig. 1a, the stress-strain curve usually exhibits discontinuous yielding behavior, as the one shown in Fig. 2a. For a steel with a microstructure containing M/A, such as the microstructure shown in Fig. 1b, the yielding behavior of the steel changes from discontinuous to continuous, and the stress-strain curve has a more "round house" appearance, as that shown in Fig. 2b. M/A could also have significant effects on other mechanical properties. In general, coarse M/A islands with a twinned martensite structure negatively affects toughness. On the other hand, a fine and

Figure 1

**Microstructures of A572-50 (a) and a weathering grade (b). Note that the brownish phase in micrograph (b) is M/A, the dark phase is pearlite, and the light-colored phase is polygonal ferrite.**

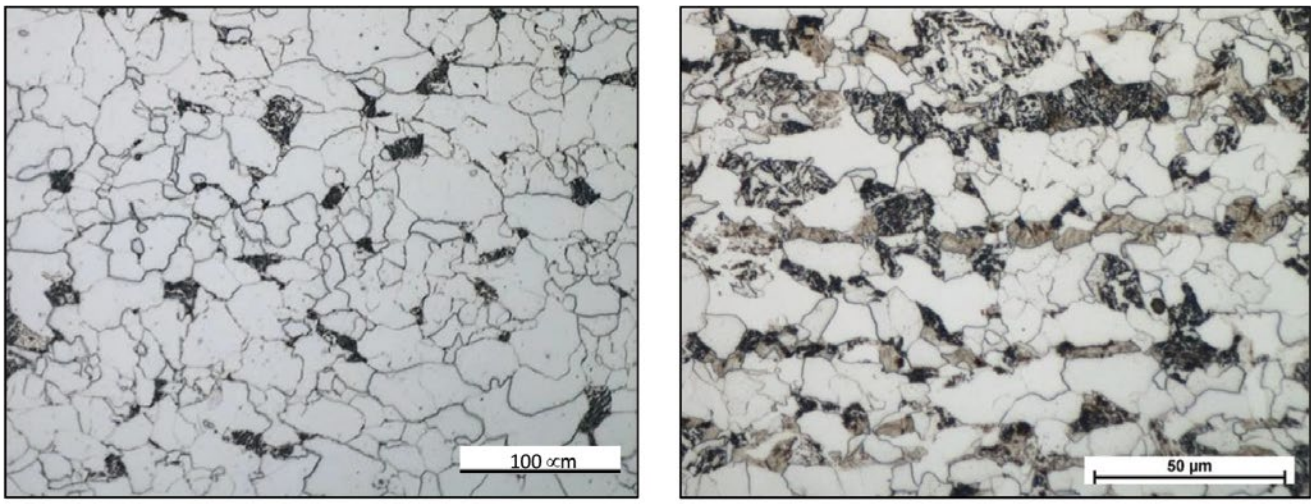


(a) (b)

Figure 2

**Tensile stress-strain curves of the two steels shown in Fig. 1: Stress-strain curve of A572-50 (a) and stress-strain curve of a weathering grade (b).**

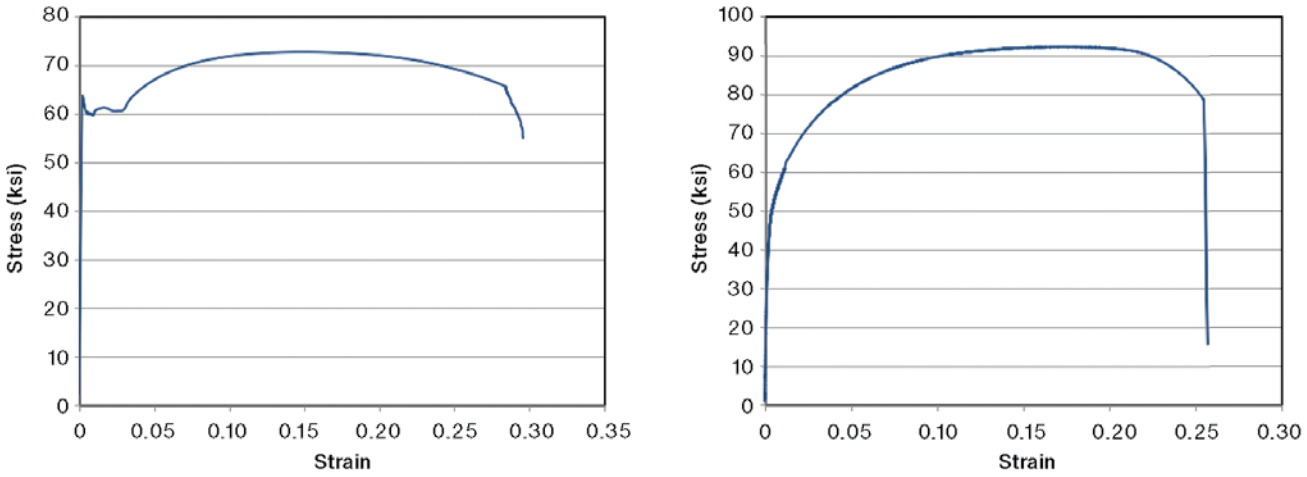


(a) (b)

uniformly distributed M/A constituent produces a lower yield-to-tensile strength (Y/T) ratio and improved uniform elongation. It is important to know how steel chemistry and the rolling process affect the formation of M/A to achieve optimal mechanical properties. To shed more light on the effects of M/A on the mechanical properties of steel, several steel plates produced for A871-65, A572-60, and API 2H-50 were examined and are presented in this article.

## Characterization of M/A

As a second phase, the volume fraction of M/A in the microstructure of a steel is relatively low and very often coexists with pearlite. This makes the characterization of this phase very difficult. With an ordinary black-and-white light optical microscope (LOM), the color of M/A is similar to that of pearlite, therefore, it can be easily overlooked in a microstructure analysis. With a color LOM,

Figure 3

**Micrographs produced using different techniques to show M/A: light optical microscopy (LOM) (2% Nital etched) (a), LOM (color etched) (b), scanning electron microscopy (SEM) (2% Nital etched) (c) and transmission electron microscopy (TEM) (bright field image) (d).**

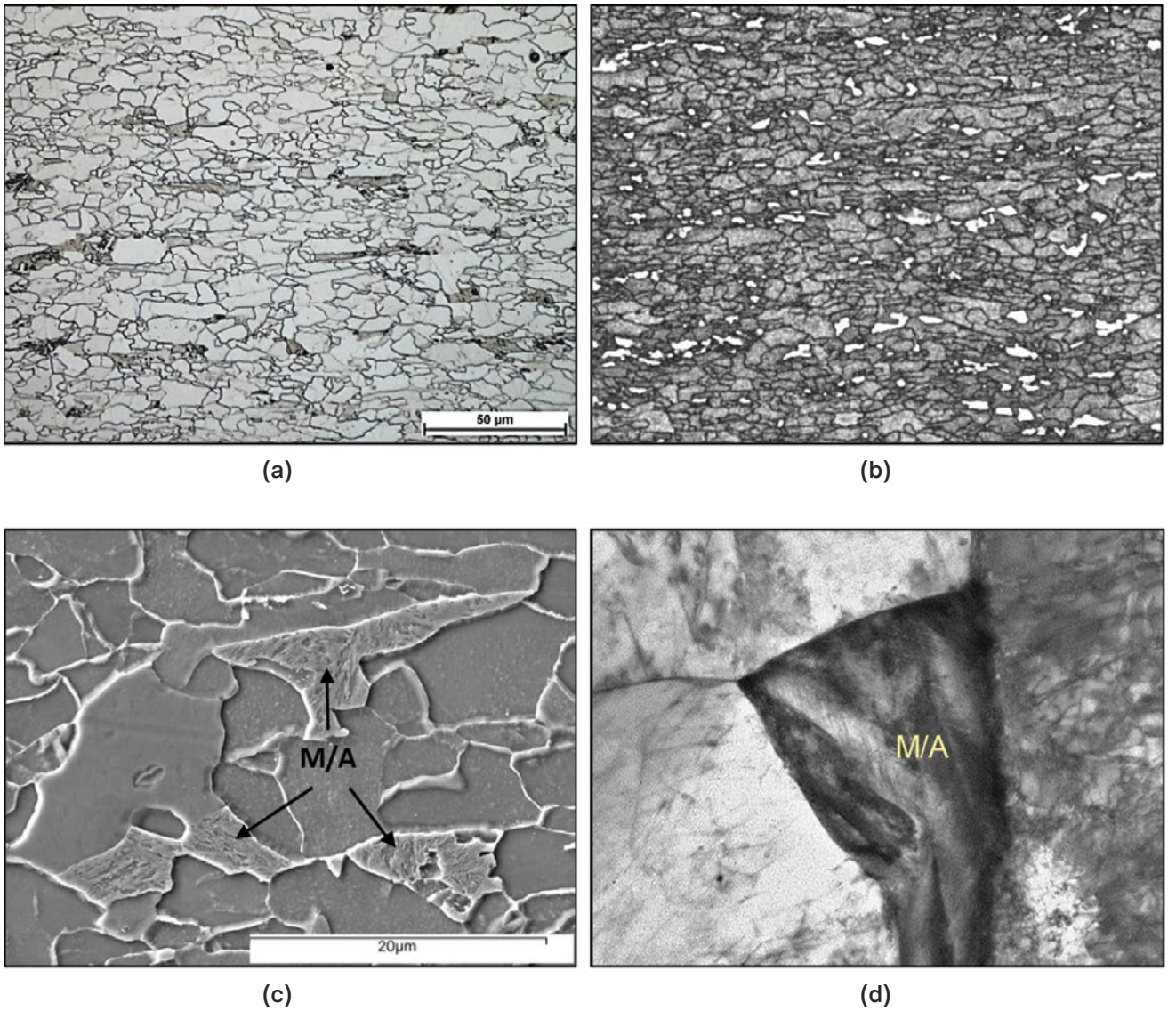


it is possible to distinguish M/A from pearlite. As shown in Fig. 3a, pearlite is the dark (or black) phase, while M/A is the brownish phase. Although this is quite helpful in a quick screening to determine if any M/A is present or not in a microstructure, it does not provide an accurate quantitative analysis of M/A since there is still a possible mix-up between M/A and pearlite. A more reliable technique for quantitative analysis on M/A is the Le Pera etching, or color etching. An example of the micrograph etched with this etchant is shown in Fig. 3b. In this micrograph, M/A is shown as the white phase. This makes quantitative analysis possible due to the excellent contrast between the phases. However, the etching itself is very challenging. The etching results depend on the quality of sample preparation and etching conditions. There are a few other techniques that have also been used to characterize M/A, such as scanning electron microscope (SEM) and transmission electron microscope (TEM). An example of a micrograph taken from an SEM is shown in Fig. 3c. In this micrograph, the islands with a rough surface constitute M/A phase. An example of the micrograph taken from a TEM is shown in Fig. 3d. In this micrograph, the dark island with twinned martensite visible constitutes M/A phase. More recently, electron backscatter diffraction (EBSD) has also been used to characterize M/A phase. Although this technique is still under development, it is a promising technique since it has the potential to not

only measure the volume fraction of M/A but also the size distribution of M/A accurately.

## Mill Examples

### Control-Rolled A871-65

The first mill example is some A871-65 discrete plates produced employing controlled rolling practices. This is a weathering grade employing a medium-carbon micro-alloyed steel. The chemical composition of the steel contains 0.15C-1.25Mn-0.035Nb. The other elements, such as Si, Cu, Ni and Cr, were added to achieve a corrosion resistance index (CI) of ≥6.0, calculated in accordance with ASTM G101. This steel chemistry (or mill melt-shop practice) covers the grade in the thickness range of 0.375–0.750 inch. The tensile results of the steel produced with this steel chemistry are summarized in Fig. 4. It can be seen that for the plates with thickness ≥0.500 inch, both the yield strength (YS) and ultimate tensile strength (UTS) meet the grade requirements (YS ≥65 ksi and UTS ≥80 ksi). For the plates with thickness below 0.500 inch, however, the yield strength of the steel decreases as the product thickness decreases. A few yield strengths were actually well below the required value for the grade, although the UTS values met the grade requirement. To determine the cause(s) of the low yield strength, samples obtained from a 0.750-inch plate and 0.375-inch plate were examined. The tensile results of these plates are summarized in Table 1. It can be seen that both the YS and UTS values obtained from the 0.750-inch plate meet the

Figure 4

**Strength-plate thickness correlation of A871-65 discrete plate.**

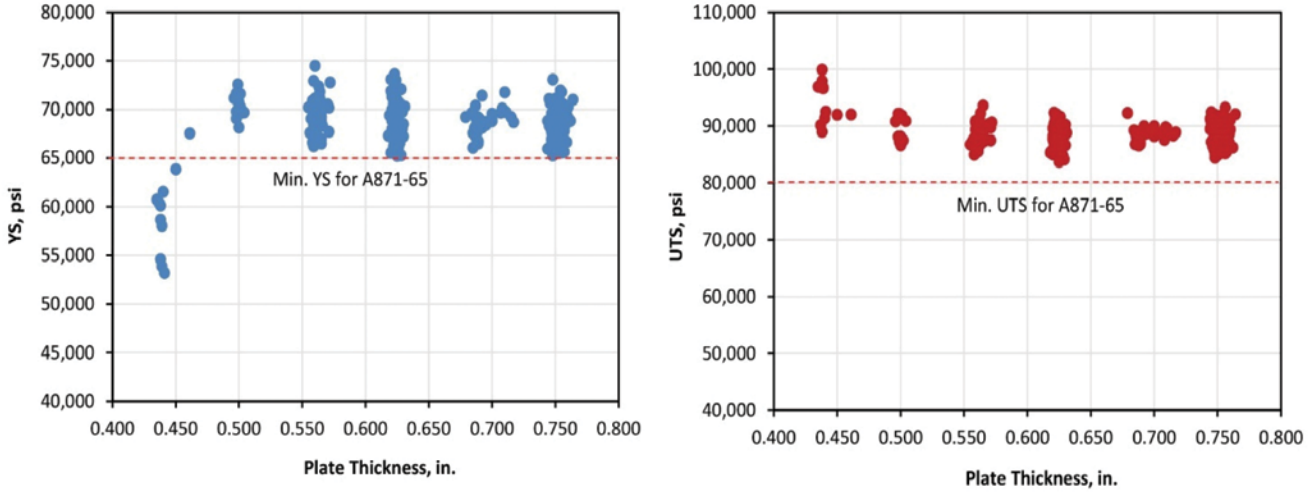


Table 1

**Mechanical Properties of A871-65**

| Plate | Thickness, inch | Yield strength, psi | Ultimate tensile strength, psi | Total elongation in 2 inch, % | Yield/ tensile ratio | Longitudinal Charpy V-Notch @ –22°F, ft-lbs |
|---|---|---|---|---|---|---|
| A | 0.750 | 70,796 | 88,500 | 30.9 | 0.80 | 88 |
| B | 0.375 | 53,883 | 98,790 | 22.2 | 0.55 | 29 |
| A871-65 | | ≥65,000 | ≥80,000 | ≥17 | N/A | ≥15 ft-lbs @ –20°F |

Note that 7.5 x 10 mm Charpy V-Notch (CVN) specimens were used for the 0.375-inch plate. The CVN value in the table is full-size equivalent.

Figure 5

**Stress-strain curves of A871-65 plates. The extensometer was taken off at a strain of about 0.6%, so only the early portion of the stress-strain curve is shown. Stress-strain curve of Plate A (a) and stress-strain curve of Plate B (b).**

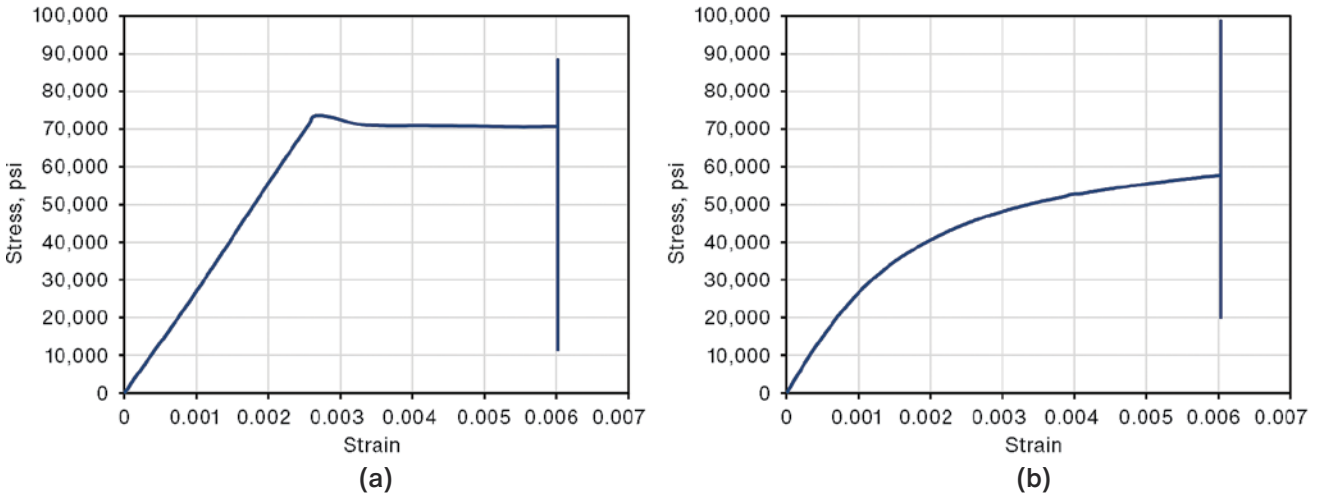


requirements for A871-65. The Charpy V-Notch (CVN) result obtained in the LRD orientation of the plate at –22°F also meets the requirement for the grade. The YS value of the 0.375-inch plate, however, is well below the requirement for the grade. The UTS value of this plate is much higher than that of the 0.750-inch plate, resulting in a much lower Y/T ratio for this plate (0.55 vs. 0.80 for the 0.750-inch plate). It can also be seen that the longitudinal Charpy V-Notch (LCVN) impact energy obtained from the 0.375-inch plate is much lower than that for the 0.750-inch plate. The tensile stress-strain curves for these two plates are shown in Fig. 5. As shown in Fig. 5a, the stress-strain curve of the 0.750-inch plate displays discontinuous yielding behavior, while that of the 0.375-inch plate exhibits continuous yielding behavior (Fig. 5b). The microstructures of these two plates are shown in Fig. 6. A color LOM was used to examine the samples. The light-color phase in these micrographs is polygonal ferrite, the dark phase is pearlite, while the brownish phase is M/A. It can be seen that the microstructure of the 0.750-inch

Figure 6

**LOM micrographs of Plate A (0.750 inch) (a) and Plate B (0.375 inch) (b).**

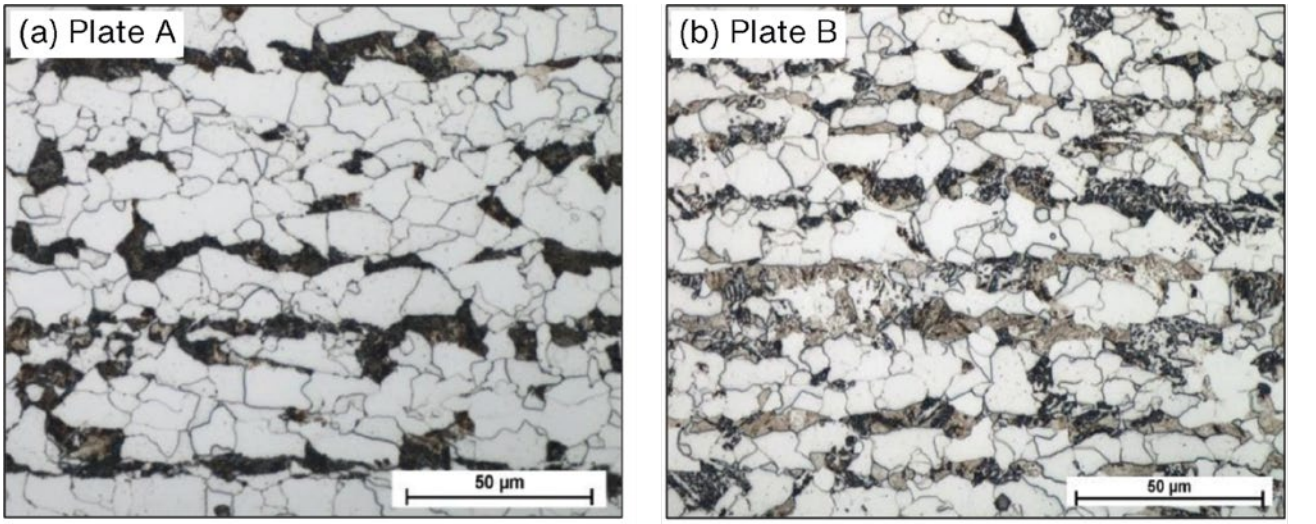

Figure 7

Scanning electron microscopy (SEM) micrographs of Plate A (0.750 inch) (a) and Plate B (0.375 inch) (b).

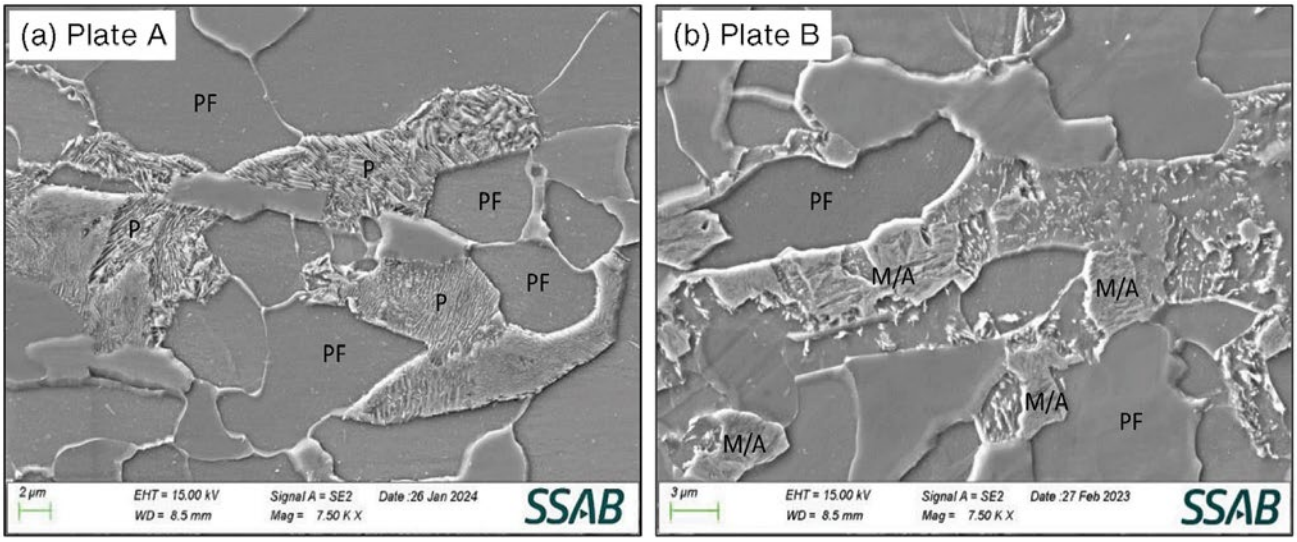


plate consists of polygonal ferrite and pearlite, while that of the 0.375-inch plate is a mixture of polygonal ferrite + pearlite + M/A. The SEM micrographs shown in Fig. 7 confirm the presence of M/A in the microstructure of the 0.375-inch plate. It is the M/A phase in the 0.375-inch plate that caused the change in yielding behavior, resulting in the low YS and high UTS values for this plate. It has been reported that an M/A volume fraction as low as 3.5% can cause a change in the yielding behavior of steel.[10] The volume fraction of M/A in Plate B (the 0.375-inch plate) is much higher than this amount, resulting in a strong effect on the yielding behavior of the steel.

To further demonstrate the effect of M/A on the mechanical properties of the steel, a sample obtained from the 0.375-inch plate was tempered at 500°C (932°F) for 30 minutes. The tensile and LCVN results obtained from this tempered sample are summarized in Table 2. For the purpose of comparison, the results obtained from the plate in the as-rolled condition are also shown in the table. The stress-strain curve of the tempered sample is shown in Fig. 8. It can be seen that the yielding behavior of the steel changed from continuous in the as-rolled condition to discontinuous in the tempered condition. The tempering treatment increased the yield strength of the steel from 53.9 ksi to 73.6 ksi (a 36.5% increase). The UTS of the steel decreased from 98.8 ksi to 91.1 ksi. The Y/T ratio increased from 0.55 to 0.81. The LCVN performance was also improved from 29 ft-lbs to 77 ft-lbs. There might be a slight boost in the yield strength from additional precipitation strengthening, assuming some

Table 2

Mechanical Properties of A871-65

| Plate | Thickness, inch | Yield strength, psi | Ultimate tensile strength, psi | Total elongation in 2 inch, % | Yield/ tensile ratio | Longitudinal Charpy V-Notch @ –22°F, ft-lbs |
|---|---|---|---|---|---|---|
| B | 0.375 | 53,883 | 98,790 | 22.2 | 0.55 | 29 |
| B-Tempered | 0.375 | 73,600 | 91,080 | 28.5 | 0.81 | 77 |
| A871-65 | | ≥65,000 | ≥80,000 | ≥17 | N/A | ≥15 ft-lbs @ –20°F |

Note that 7.5 x 10 mm CVN specimens were used for testing. The CVN values in the table are full-size equivalent.

Figure 8

**Stress-strain curves of A871-65 plates. The extensometer was taken off at a strain about 0.6%, so only the early portion of the stress-strain curves is shown. Stress-strain curve in the as-rolled condition (a) and stress-strain curve in the tempered condition (b).**

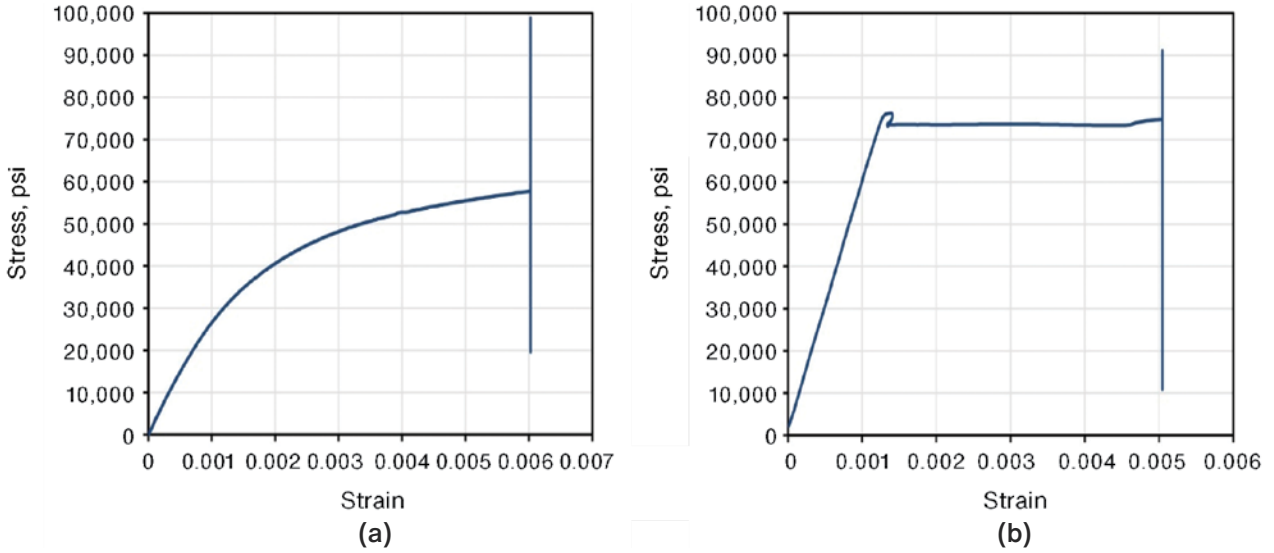


NbC precipitates formed during the tempering treatment. However, based on the significant improvement in both the strength and toughness of the steel, it is believed that the primary contributor to this improvement is M/A tempering (annihilation of dislocations). Similar effects of M/A tempering on the mechanical properties of a weathering steel have been reported previously.[11]

Figure 9

**Continuous-cooling-transformation (CCT) diagram of the medium-carbon A871-65 (calculated using JMatPro).**

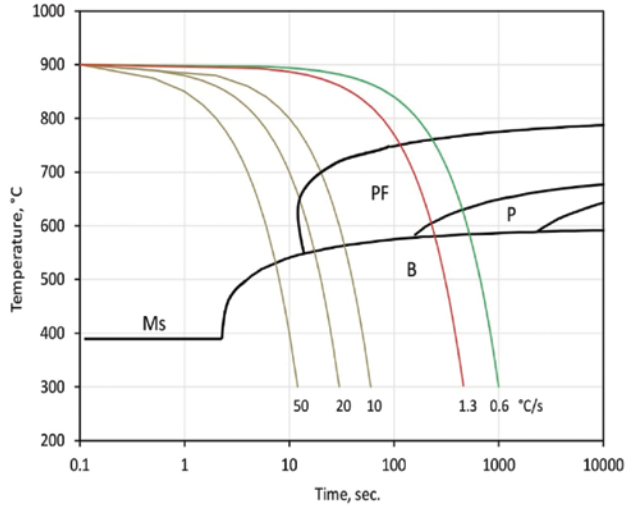


To understand what caused the difference in microstructure between the 0.375-inch and 0.750-inch plates, the continuous-cooling-transformation (CCT) diagram for the steel chemistry was calculated using JMatPro. The calculated CCT diagram is shown in Fig. 9. The estimated cooling rates for the 0.375-inch and 0.750-inch plates are about 1.3 and 0.6°C/second, respectively. The cooling curves are plotted in the CCT diagram. It can be seen that the cooling curve of the 0.750-inch plate (0.6°C/second) crossed the polygonal ferrite and pearlite phase regions, then entered the bainite phase region. Due to the relatively slow cooling rate, the final microstructure consists primarily of polygonal ferrite and pearlite. The cooling curve of the 0.375-inch plate (1.3°C/second) also crossed the polygonal ferrite and pearlite phase regions. However, the cooling curve only cuts the corner of the pearlite phase region, resulting in a lower volume of pearlite in the microstructure. In this case, a significant amount of remaining alloy-enriched austenite will transform to either bainite or M/A. The final microstructure will be a mixture of polygonal ferrite + pearlite + bainite or M/A. This explains the difference in microstructure between the 0.375-inch and 0.750-inch plates.

Based on the microstructure results, it was concluded that the M/A phase in the microstructure of the 0.375-inch plate is the primary cause of the continuous yielding behavior and low yield strength for this plate. The higher cooling rate associated with the 0.375-inch plate contributed to the formation of M/A in the microstructure of this plate. To reduce the M/A effect and boost the yield strength of the steel, the steel chemistry was modified to reduce the hardenability of the steel. A mill

Table 3

**Mechanical Properties of A871-65**

| Plate | Thickness, inch | Yield strength, psi | Ultimate tensile strength, psi | Total elongation in 2 inch, % | Yield/ tensile ratio | Longitudinal Charpy V-Notch @ –22°F, ft-lbs |
|---|---|---|---|---|---|---|
| B | 0.375 | 53,883 | 98,790 | 22.2 | 0.55 | 29 |
| C | 0.375 | 67,744 | 85,690 | 28.4 | 0.79 | 124 |
| A871-65 | | ≥65,000 | ≥80,000 | ≥17 | N/A | ≥15 ft-lbs @ –20°F |

Note that 7.5 x 10 mm CVN specimens were used for testing. The CVN values in the table are full-size equivalent.

trial was conducted using the modified steel chemistry and the results are shown in Table 3. Plate B is the plate produced with the original steel chemistry, while Plate C is the trial plate produced using the modified steel chemistry. It can be seen that the yield strength of Plate C was improved significantly and met the requirements for the grade. It is also interesting to see that the Y/T ratio of the steel increased from 0.55 to 0.79 and the LCVN impact energy was also much higher for the plate produced with the modified steel chemistry. The tensile stress-strain curve, LOM and SEM micrographs are shown in Figs. 10–12, respectively. For the purpose of comparison, the stress-strain curve obtained from the 0.375-inch plate produced with the original steel chemistry is shown in Fig. 10a. It can be seen that the yielding behavior of the steel changed from continuous to discontinuous by reducing the steel hardenability. This is mainly due to the elimination of the M/A constituent in the microstructure of Plate C, as shown by the micrographs in Figs. 11 and 12.

## Control-Rolled A572-60

The second mill example is control-rolled A572-60. Two steel chemistries were used to produce the grade. As shown in Table 4, the contents of C, Si, Cr and Mo of Plate E are higher than those of Plate D. The steel chemistry for Plate D is in accordance with the standard meltshop practice (MSP) for A572-60. The steel chemistry for Plate E did not meet the MSP requirements due to high concentrations of Si and Cr, but the concentrations of these elements were within the chemical requirements for the grade. The tensile and LCVN results obtained from both plates are shown in Table 5. It can be seen that the strengths of both plates meet the requirement

Figure 10

**Stress-strain curves of A871-65 plates: Plate B (a) and Plate C (b).**

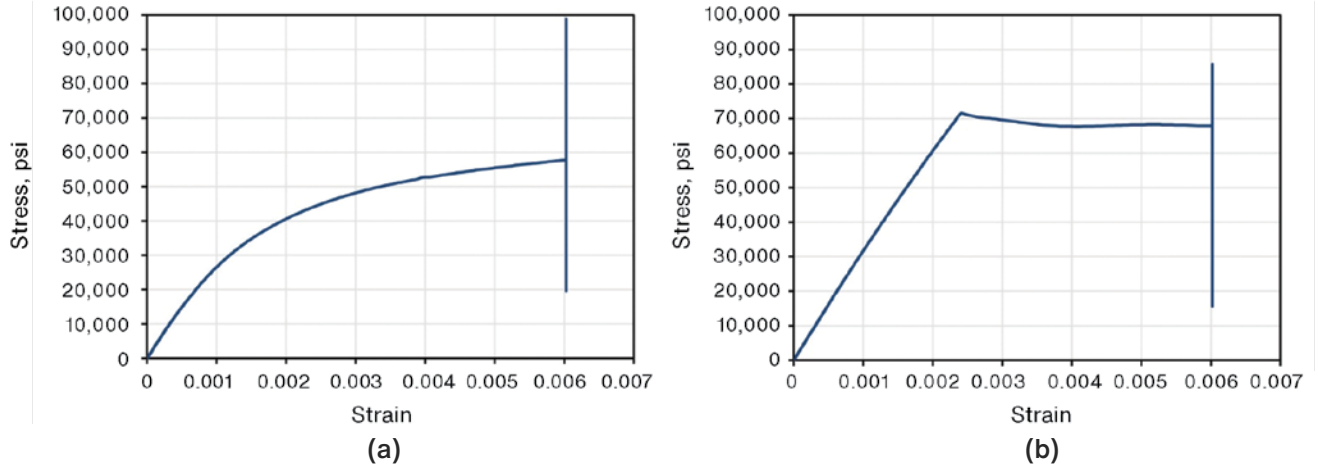

Figure 11

LOM micrographs of Plate B (original chemistry) (a) and Plate C (modified chemistry) (b).

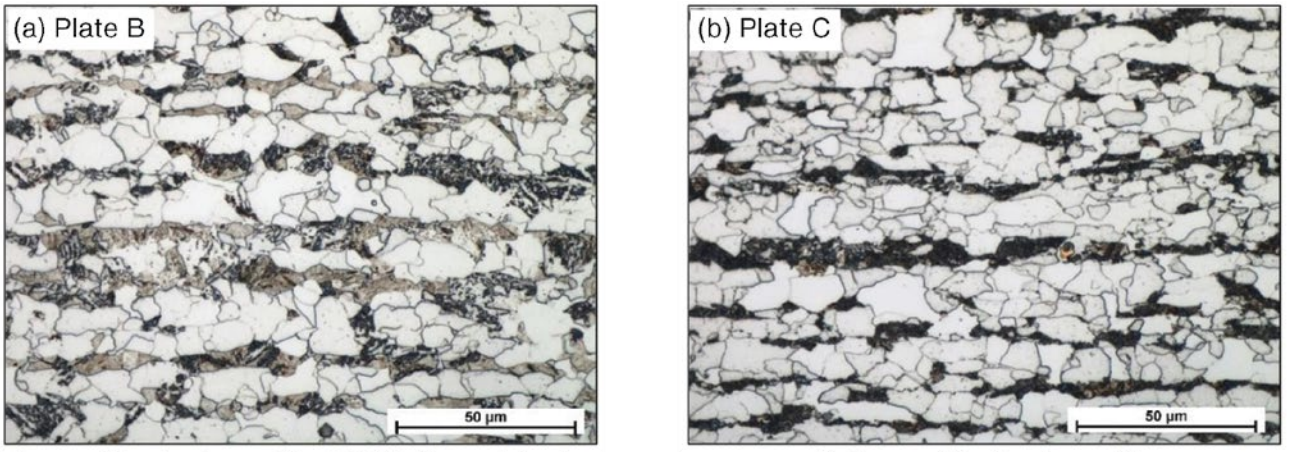


Polygonal ferrite + pearlite + M/A (brownish phase)

Polygonal ferrite + pearlite

Figure 12

SEM micrographs of Plate B (original chemistry) (a) and Plate C (modified chemistry) (b).

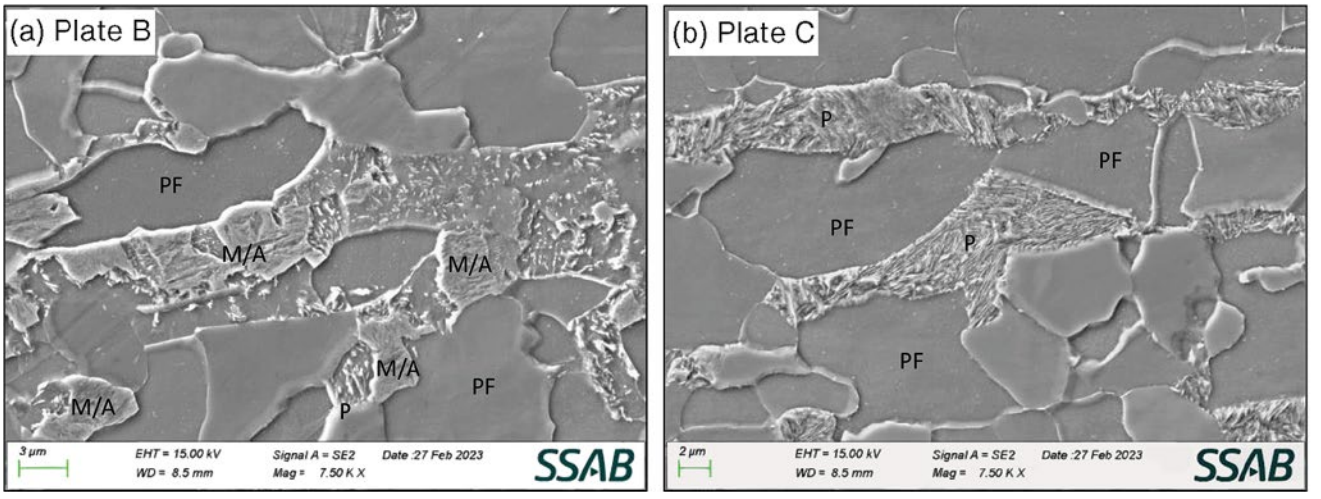


Table 4

Chemical Compositions of the Steels, wt. %

| Plate | C | Si | Cr | Mo | Mn, Cu, Ni, Nb, V, Ti |
|---|---|---|---|---|---|
| D | 0.158 | 0.06 | 0.12 | 0.03 | Same for the heats |
| E | 0.165 | 0.23 | 0.28 | 0.05 | |

for A572-60. The UTS value of Plate E is much higher than that of Plate D, resulting in a significantly lower Y/T ratio for Plate E. The LCVN impact energy of Plate E is also noticeably lower than that of Plate D. The tensile stress-strain curves of these plates are shown in Fig. 13. It can be seen that the stress-strain curve of Plate D displays discontinuous yielding behavior, while the stress-strain curve of Plate E exhibits continuous yielding behavior. Similar to the observation from the A871-65 plates presented earlier, the M/A constituent in the microstructure of

Table 5

**Mechanical Properties of A572-60**

| Plate | Thickness, inch | Yield strength, psi | Ultimate tensile strength, psi | Yield/ tensile ratio | Longitudinal Charpy V-Notch @ –22°F, ft-lbs |
|---|---|---|---|---|---|
| D | 1.000 | 71,850 | 92,090 | 0.78 | 57 |
| E | 0.750 | 68,480 | 116,990 | 0.59 | 21 |

Plate E is likely the cause of the yielding behavior change.

The LOM and SEM micrographs of these plates are shown in Figs. 14 and 15. The microstructure of Plate D consists of polygonal ferrite and pearlite, while the microstructure of Plate E is a mixture of polygonal ferrite + pearlite + bainite + M/A. The presence of a

Figure 13

**Stress-strain curves of A572-60 plates: Stress-strain curve of Plate D (1.0 inch) (a) and stress-strain curve of Plate E (0.750 inch) (b).**

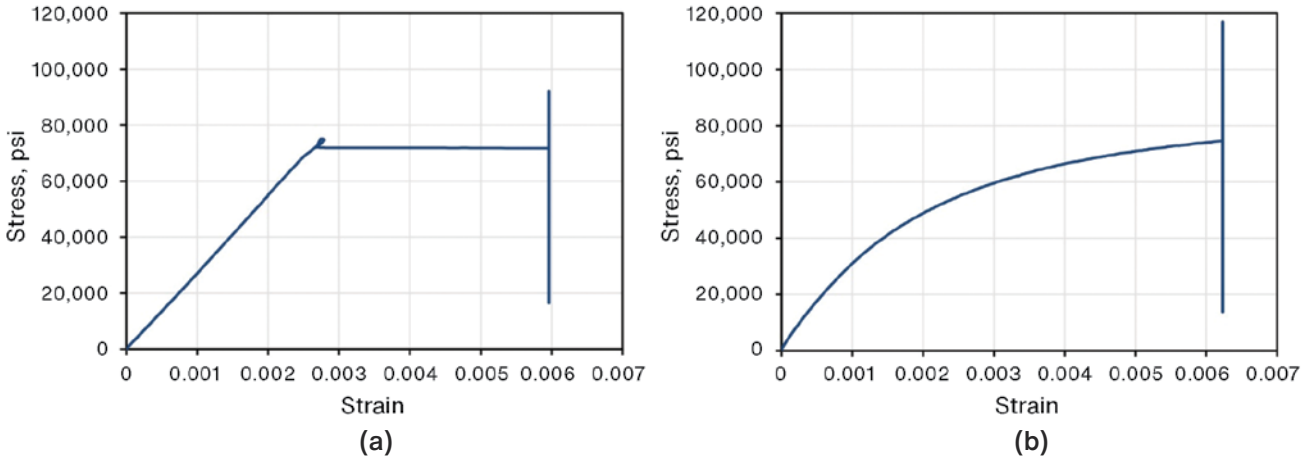


Figure 14

**LOM micrographs of A572-60.**

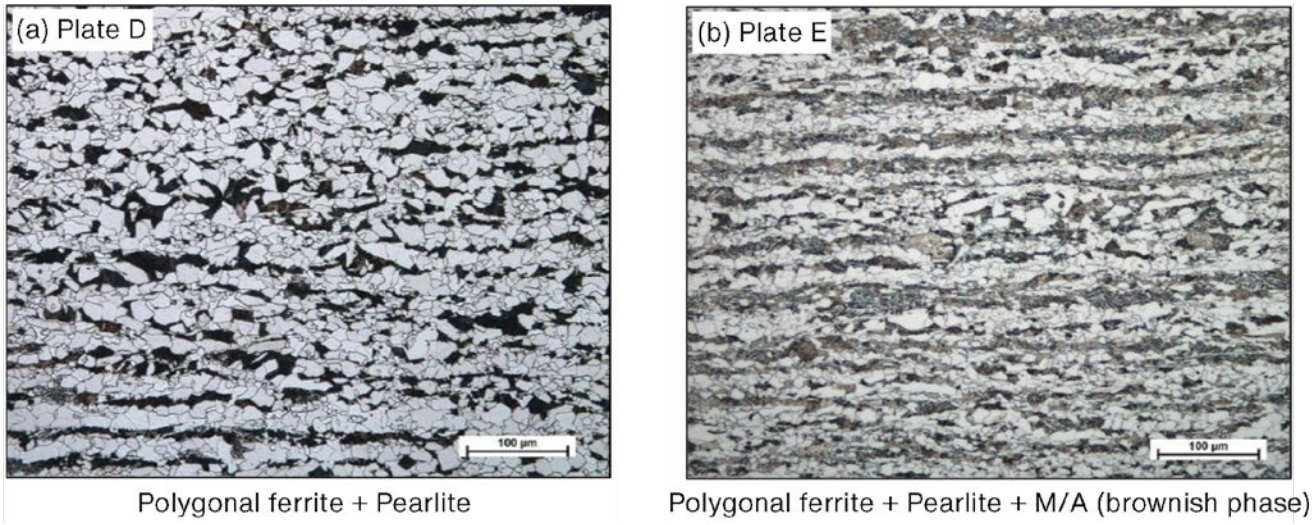

Figure 15

SEM micrographs of A572-60.

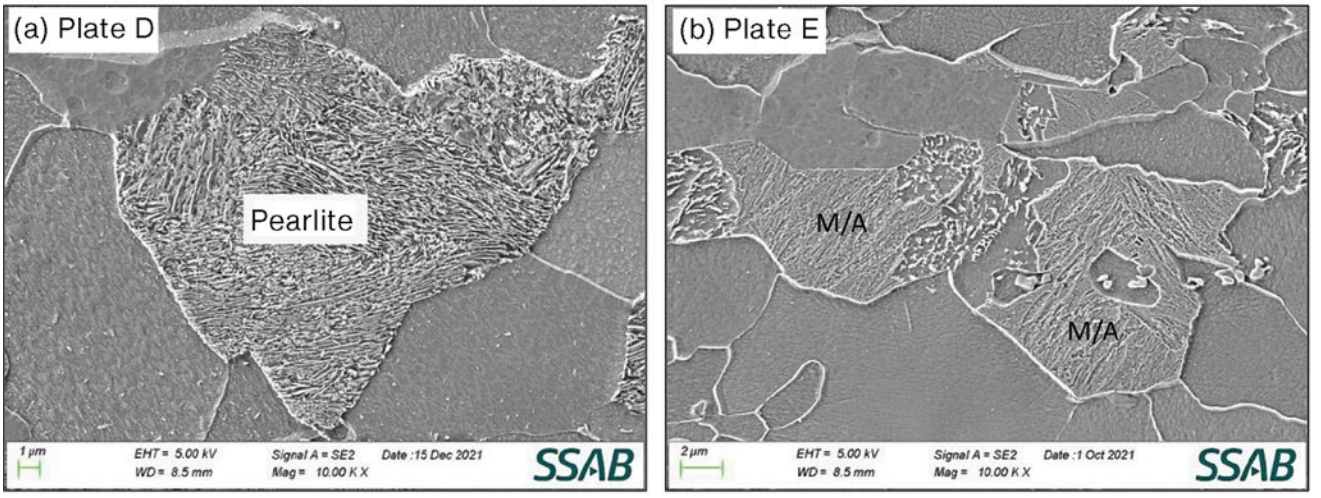


significant amount of M/A in the microstructure of Plate E is the primary cause of the lower yield strength and higher UTS for this plate. The M/A constituent in the microstructure of this plate is also the cause of the lower CVN impact energy obtained for this plate. The higher C, Cr and Mo in the heat used for Plate E increased the hardenability of the steel, thereby promoting the formation of bainite and M/A. The higher Si in the heat likely played a role in suppressing the formation of pearlite, which also contributed to the formation of the M/A constituent. This together with the A871-65 example shown earlier indicates that M/A could form in many steel products. The presence of M/A phase could have significant negative effects on the mechanical properties of steel. Steel chemistry and rolling process, especially the cooling rate after finish rolling, need to be closely controlled in order to prevent a significant amount of M/A constituent in the microstructure of a steel product.

## Normalized API 2H-50

The third mill example is normalized API 2H-50. The steel chemistry used for this grade is a medium-carbon Mn steel with a small addition of Nb for grain size control. In the original chemistry design, a small amount of Mo (0.06 wt. %) was added to improve the margin for meeting the UTS requirement of the steel. This steel chemistry worked for plate thicknesses over 0.375 inch. For light-gauge products, such as 0.250-inch plate, this steel chemistry produced failing yield strength for the grade. To determine the cause(s) of the failure, a heat with a lower Mo content was made for a trial. Several plates produced from this heat together with those from a higher Mo heat were examined. As shown in Table 6, the only major difference between these two heats is the Mo content. In heat A, the Mo content was 0.067 wt. %. In heat B, the Mo content was reduced to 0.042 wt. %. This appears to be only a small change in steel chemistry. Its effect on the mechanical properties of the steel is quite dramatic, as shown by the tensile and LCVN results presented in Table 7. It can be seen that the yield strength of the steel was increased by almost 14 ksi, while the UTS of the steel was decreased by 6 ksi. The Y/T ratio was increased from 0.57 to 0.77. The CVN impact energy was increased from 54 to 103 ft-lbs (almost a 100% increase). The tensile stress-strain curves for these two plates are shown in Fig. 16. It can be seen that the yielding behavior of the steel changed from continuous for the 0.067 Mo heat to discontinuous for the 0.042 Mo heat. This suggests that the microstructures for these two plates could be very different.

The LOM and SEM micrographs of these plates are shown in Figs. 17 and 18. The microstructure of the plate produced from heat A (the 0.067 Mo heat) is a mixture of polygonal ferrite + pearlite + M/A, while the microstructure of the plate produced from heat B (the 0.042 Mo heat) consists of polygonal ferrite and pearlite. The presence of a significant amount of M/A in the microstructure of the plate produced from heat A is the primary

Table 6

Chemical Compositions of the Steels, wt. %

| Heat # | C | Mo | Mn, Cu, Ni, Nb, V, Ti |
|---|---|---|---|
| A | 0.120 | 0.067 | Same for the two heats |
| B | 0.118 | 0.042 | |

Table 7

**Mechanical Properties of 2H-50**

| Heat # | Thickness, inch | Yield strength, psi | Ultimate tensile strength, psi | Total elongation in 2 inch, % | Yield/ tensile ratio | Transverse Charpy V-Notch @ –50°F, ft-lbs |
|---|---|---|---|---|---|---|
| A | 0.250 | 48,100 | 86,140 | 31.8 | 0.57 | 54 |
| B | 0.250 | 62,200 | 79,920 | 34.4 | 0.77 | 103 |
| API 2H-50 | | ≥50,000 | ≥70,000 | ≥21.0 | N/A | ≥30 @ –40°F |

*5 mm CVN specimens were used for testing, the values in the table are full-size equivalent values

cause of the lower yield strength and higher UTS for this plate. The M/A constituent in the microstructure of this plate is also the cause of the lower CVN impact energy obtained for this plate. The higher Mo content in the heat increased the hardenability of the steel, thereby promoting the formation of M/A phase. It should be pointed out that in a steel without Nb addition, the effect of Mo at a residual level is not as strong as the observation in steels with Nb addition. It is well known that the effects of Nb and Mo on the austenite-to-ferrite transformation are similar. Both elements retard the phase transformation, and in particular the transformation of austenite to pearlite, thus promoting bainite or M/A phase formation. It appears that there is a synergetic effect of Nb and Mo on the M/A formation. In other words, with the presence of Nb in a steel, the effect of Mo on the M/A formation is exaggerated. This is not well understood; therefore, this requires further study.

## Summary

The presence of M/A constituent in the microstructure of steel can significantly affect the mechanical properties of steel. It is important to know how steel chemistry and processing condition affect the formation of M/A phase, thereby achieving optimal mechanical properties. To demonstrate the effects of M/A on the mechanical properties of medium-carbon microalloyed steels, several mill examples were investigated. For A871-65, at a relatively high air cooling rate (1.3°C/second), a significant amount of M/A was introduced in the microstructure of the steel. This changed the yielding behavior of the steel from discontinuous to continuous, resulting in low yield strength and high UTS. The presence of M/A phase also negatively affected the toughness of the steel. By decreasing the hardenability of the steel, the volume fraction of M/A constituent was effectively reduced or eliminated. This improved both the yield strength and toughness of

Figure 16

**Stress-strain curves of 2H-50 plates: Stress-strain curve of Heat A (a) and stress-strain curve of Heat B (b).**

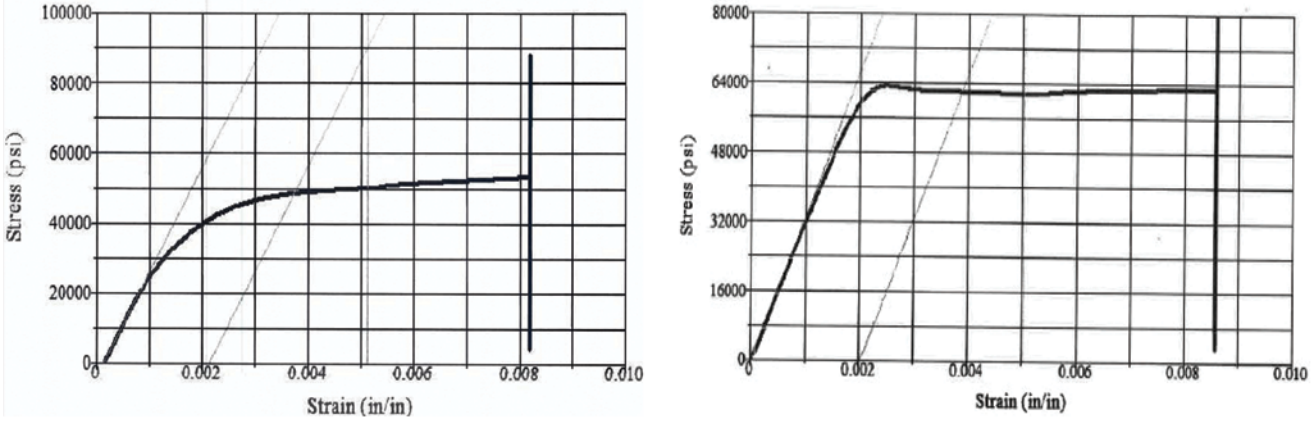

Figure 17

LOM micrographs of 2H-50.

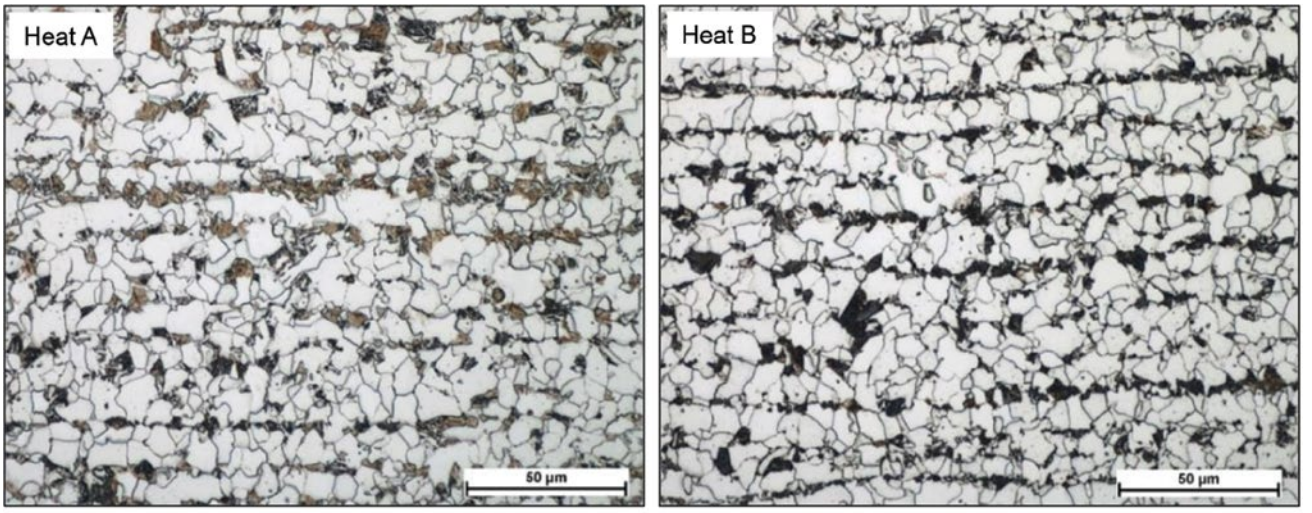


Polygonal Ferrite + + M/A (brownish phase)

Polygonal Ferrite + Pearlite

Figure 18

SEM micrographs of 2H-50.

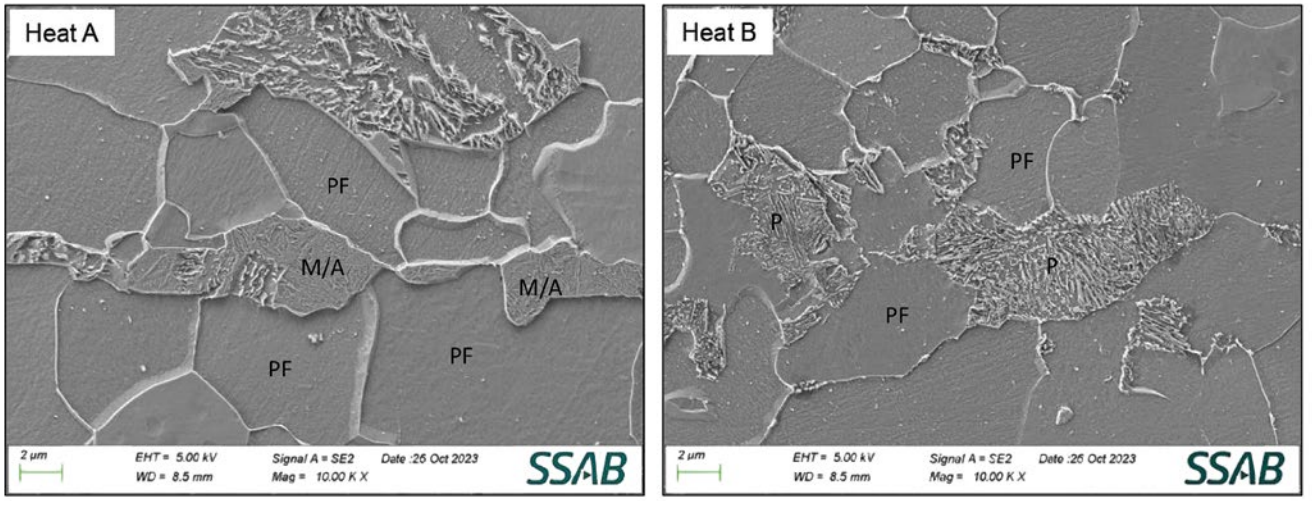


the steel. It was also demonstrated that chemical composition of steel can significantly affects the volume fraction of M/A constituent, thereby mechanical properties of grades A572-60 and API 2H-50. As shown in this article, at a very low level, Mo could have a strong effect on the formation of M/A phase, and hence the mechanical properties of steel. This is particularly true when Nb is present in a steel, which showed that there is a synergetic effect of Nb and Mo on the formation of M/A phase. This is not well understood; therefore, this requires further studies.

## Acknowledgments

The authors would like to thank rolling mill personnel and test lab staff at SSAB Americas for their great support in conducting mill trials and providing test data. The authors are also grateful to Rick Bodnar and Sunday Abraham for their critical review of the manuscript, and the SSAB Americas senior management for their permission to publish this work.

## References


1. J.M Rigsbee and P.J. VanderArend, *Formable HSLA and Dual-Phase Steels,* A.T. Davenport, ed., October 1977, pp. 56–86.
2. A.P. Coldren, G. Tither, A. Cornford and J.R. Hiam, *Formable HSLA and Dual-Phase Steels,* A.T. Davenport, ed., October 1977, pp. 205–227.
3. G.R. Speich, A.J. Schwoeble and G.P. Huffman, *Metallurgical Transactions A,* Vol. 14A, 1983, pp. 1079–1087.
4. Y. Sakuma, D.K. Matlock and G. Krauss, "Intercritically Annealed and Isothermally Transformed 0.15 pct C Steels: Part 1. Transformation, Microstructure, and Room Temperature Mechanical Properties," *Metallurgical Transactions of the ASME,* Vol. 23A, April 1992, pp. 1221–1231.
5. T. Senuma, "Physical Metallurgy of Modern High Strength Steel Sheets," *ISIJ International,* Vol. 41, No. 6, 2001, pp. 520–532.
6. N. Ishikawa, M. Okatsu and S. Endo, J. Kondo, "Design Concept and Production of High Deformability Linepipe," *Proceedings of the 6th International Pipeline Conference,* Calgary, Canada, 2006, IPC2006-10240.
7. D.H. Seo, C.M. Kim, J.Y. Yoo and K.B. Kang, "Microstructure and Mechanical Properties of X80/X100 Grade Plates and Pipes," *Proceedings of the 7th International Offshore and Polar Engineering Conference, ISOPE-2007,* Lisbon, Portugal, 2007, pp. 3301–3306.
8. M. Liebeherr, D.R. Romera, B. Soenen, S. Ehlers and E. Hivert, "Recent Developments of High Strength Linepipe Steels on Coil," *Proceedings of the 7th International Pipeline Conference,* Calgary, Canada, 2008, IPC2008-64295.
9. T. Hara and T. Fujishiro, *Proceedings of the 8th International Pipeline Conference,* Calgary, Canada, 2010, IPC2010-31166.
10. D. Bai, E. Lynch, C. Rawlinson, R. Bodnar and S. Thompson, *2nd International Symposium on the Recent Developments in Plate Steels,* 2018, pp. 231–244.
11. D. Bai, T. Nelson, R. Bodnar, S. Scumpu and M. Cooke, *MS&T 2008 Conference Proceedings,* 2008, pp. 1312–1324. ✦


AISTech This paper was presented at AISTech 2024 — The Iron & Steel Technology Conference and Exposition, Columbus, Ohio, USA, and published in the AISTech 2024 Conference Proceedings.